



Cite this: *Phys. Chem. Chem. Phys.*,
2015, 17, 7966

Towards efficient photoinduced charge separation in carbon nanodots and TiO₂ composites in the visible region†

Mingye Sun,^{ab} Songnan Qu,^{*a} Wenyu Ji,^a Pengtao Jing,^a Di Li,^a Li Qin,^a
Junsheng Cao,^a Hong Zhang,^c Jialong Zhao^a and Dezhen Shen^{*a}

In this work, photoinduced charge separation behaviors in non-long-chain-molecule-functionalized carbon nanodots (CDs) with visible intrinsic absorption (CDs-V) and TiO₂ composites were investigated. Efficient photoinduced electron injection from CDs-V to TiO₂ with a rate of $8.8 \times 10^8 \text{ s}^{-1}$ and efficiency of 91% was achieved in the CDs-V/TiO₂ composites. The CDs-V/TiO₂ composites exhibited excellent photocatalytic activity under visible light irradiation, superior to pure TiO₂ and the CDs with the main absorption band in the ultraviolet region and TiO₂ composites, which indicated that visible photoinduced electrons and holes in such CDs-V/TiO₂ composites could be effectively separated. The incident photon-to-current conversion efficiency (IPCE) results for the CD-sensitized TiO₂ solar cells also agreed with efficient photoinduced charge separation between CDs-V and the TiO₂ electrode in the visible range. These results demonstrate that non-long-chain-molecule-functionlized CDs with a visible intrinsic absorption band could be appropriate candidates for photosensitizers and offer a new possibility for the development of a well performing CD-based photovoltaic system.

Received 24th January 2015,
Accepted 16th February 2015

DOI: 10.1039/c5cp00444f

www.rsc.org/pccp

Introduction

Carbon-based nanomaterials, including fullerene, graphene, carbon nanotubes, and carbon nanodots (CDs), have been regarded as a viable alternative to organic dyes and traditional semiconductor quantum dots (QDs) in bioimaging and biosensing, photocatalysis, optoelectronics, and photovoltaics (PVs).^{1–8} Especially, CDs, owing to their superior performance in terms of water solubility, stability, toxicity, resistance to photobleaching, and biocompatibility, have recently drawn significant attention.^{9–15} The electron injection from CDs to TiO₂ was demonstrated to be feasible and the CD-sensitized TiO₂ photoelectrodes have been applied in photocatalysis and PVs.^{10,16–21} However, it is still a challenge to achieve efficient electron injection from CDs to TiO₂ under sunlight,²¹ which is a primary

photophysical process in generating photocurrent in CD-based PVs.^{22,23} To date, the power conversion efficiency of CD-based PVs has been only 0.13%, as reported by Mirtchev and co-workers.²¹ The authors pointed out that the low power conversion efficiency was possibly due to inferior electron injection from CDs to TiO₂. Most of the CDs, such as those prepared by laser ablation, electrochemical oxidation, and hydrothermal synthesis, have the main absorption band in the ultraviolet region,¹⁰ which is unfavorable for efficient absorption of solar energy. The CDs used by Mirtchev *et al.* in the CD-based PVs have absorption bands mainly in the ultraviolet region with a tail in the visible region.²¹ The long tail absorption band possibly arises from surface defect states.^{24,25} The surface defects are unstable and dissipative in energy, which are unfavorable for efficient electron injection in PVs.^{23,26–28} In addition, the reported CDs are generally passivated with insulating long chain molecules,^{10,12,29} which act as tunneling barriers and are against efficient electron injection and well performing CD-based optoelectronic devices.^{22,30} To realize efficient CD-sensitized TiO₂ PVs under sunlight, the CDs should exhibit intrinsic absorption in the visible region and be integrated effectively with TiO₂. Thus, it is of significant interest to exploit such photoelectrodes based on CD/TiO₂ composites to demonstrate the possibility of developing a well performing CD-based PV system.

Previously, we prepared non-long-chain-molecule-functionlized CDs with a strong and specific absorption band in the visible region (CDs-V) extending to 500 nm, which exhibited superior

^a State Key Laboratory of Luminescence and Applications, Changchun Institute of Optics, Fine Mechanics and Physics, Chinese Academy of Sciences, 3888 Eastern South Lake Road, Changchun, Jilin 130033, China. E-mail: qusn@ciomp.ac.cn, shendz@ciomp.ac.cn

^b University of Chinese Academy of Sciences, Beijing 100039, China

^c Van't Hoff Institute for Molecular Sciences, University of Amsterdam, Science Park 904, 1098 XH Amsterdam, The Netherlands

† Electronic supplementary information (ESI) available: Measurement section. Optical images of pure TiO₂ and CDs-V/TiO₂ composites. The normalized absorption spectra of RhB solution and RhB solutions mixed with CDs-V, pure TiO₂, CDs-U/TiO₂ and CDs-V/TiO₂ composites after different visible light irradiation times. The normalized absorption spectra of CDs-U and CDs-V. See DOI: 10.1039/c5cp00444f

photostability compared with organic dyes.^{12,29,31,32} Amplified spontaneous green emission and lasing were achieved from the CDs-V.²⁹ Green photoluminescence (PL) was proposed to be intrinsic state emission and the visible absorption was from intrinsic absorption rather than from surface defect states.²⁹ In this work, we demonstrated that the CDs-V could be integrated with TiO₂ with the absorption band extending to the visible region. Efficient photoelectrodes were prepared by integrating the CDs-V with the TiO₂ film on the fluorine-doped tin oxide (FTO) substrate with fast and efficient electron injection from CDs-V to TiO₂ with a rate of $8.8 \times 10^8 \text{ s}^{-1}$ and an efficiency of 91%. The electron injection properties and charge separation processes for the CDs-V/TiO₂ composites were investigated through regulating the surrounding environment. The CDs-V/TiO₂ composites exhibited excellent photocatalytic activity under visible light, much better than pure TiO₂ and the CDs with the main absorption band in the ultraviolet region (CDs-U) and TiO₂ composites, indicating that visible photoinduced electrons and holes in CDs-V/TiO₂ composites could be effectively separated. The CD-sensitized TiO₂ solar cells were prepared. The incident photon-to-current conversion efficiency (IPCE) results also agreed with efficient charge separation between CDs-V and the TiO₂ electrode in the visible range. These interesting results demonstrate that the non-long-chain-molecule-functionized CDs with visible intrinsic absorption could be appropriate photosensitizers and offer new opportunities for developing a well performing CD-based PV system.

Experimental section

Chemicals and materials

Citric acid (99.5%) and urea (99%) were purchased from Beijing Chemical Works. TiO₂ powder (P25, a mixed phase of 80% anatase and 20% rutile; average size 25 nm) was purchased from Degussa. CdSe/ZnS core/shell QDs were purchased from Ocean Nano Tech LLC. All chemicals were used without further purification. The water used in all experiments was purified using a Millipore system.

Synthesis of CDs-V

3 g of citric acid and 6 g of urea were added to 20 mL of deionized water to form a transparent solution. Then the mixed solution was heated in a domestic 750 W microwave oven for about 5 minutes, during which the solution changed from a colorless liquid to a light brown and finally dark brown clustered solid, indicating the formation of CDs. The solid was then dissolved in water and centrifuged to remove agglomerated particles with a speed of 8000 rpm for 20 min three times.

Synthesis of CDs-U

3 g of citric acid and 6 g of urea were added to 20 mL of deionized water to form a transparent solution. The mixed solution was transferred into a 50 mL Teflon-lined stainless-steel autoclave. Then the sealed autoclave was heated to 160 °C and kept for about 4 h.

Fabrication of CD/TiO₂ composites

The CD/TiO₂ composites were prepared by simply dispersing P25 powder in CDs-U or CDs-V aqueous solution (5 mg mL^{-1}) with constant stirring for 24 h. All the reaction mixtures were washed with water and centrifuged to remove unadsorbed CDs with a speed of 5000 rpm until the supernatant was non-fluorescent. The samples were then dried at 80 °C and kept in a vacuum oven for further experiments and measurements. The color of TiO₂ changes from pure white to light brown after integrating with the CDs-V as shown in Fig. S1 (ESI†).

Fabrication of CDs-V/TiO₂ composites on glass and FTO substrates

The TiO₂ films were spread on glass and FTO substrates by spin-coating P25 paste onto the substrates with a speed of 2500 rpm for 60 s, and the obtained substrates were calcined at 500 °C in air for 60 min and cooled to room temperature naturally. The TiO₂ films on glass and FTO substrates were immersed in the aqueous solution of CDs-V with a concentration of 5 mg mL^{-1} for 24 h and then rinsed thoroughly with water.

Fabrication of CD-sensitized solar cells

TiO₂ mesoporous films were spread on FTO substrates by successive screen printing of P25 paste as the transparent layer ($9.5 \pm 0.5 \text{ }\mu\text{m}$) and 30 wt% 200–400 nm TiO₂ mixed with 70 wt% P25 paste as the light scattering layer ($6.5 \pm 0.5 \text{ }\mu\text{m}$). The obtained substrates were calcined at 500 °C in air for 60 min and cooled to room temperature naturally. A modification of the TiO₂ mesoporous films with an aqueous solution of TiCl₄ (0.04 M) was then performed. For the integration of CDs-V with TiO₂ film electrodes, the TiO₂ mesoporous films on FTO substrates were immersed in the aqueous solution of CDs-V with a concentration of 5 mg mL^{-1} for 24 h and then rinsed thoroughly with water. Platinum coated FTO was chosen as the counter electrode. The solar cells were prepared by sealing the platinum coated FTO counter electrode and CD-sensitized TiO₂ film electrode with a binder clip using a Scotch spacer. Then, a small amount of I^-/I_3^- electrolyte was infiltrated into the cell through a pre-drilled hole in the platinum coated FTO counter electrode.

Photocatalytic activity measurements

The photocatalytic activity of the samples was tested through measuring the decomposition rate of Rhodamine B (RhB) molecules under visible light irradiation ($\lambda > 400 \text{ nm}$) from a Zolix SS150 solar simulator with a 400 nm cut-off filter. The CDs-V, P25 TiO₂, CDs-U/TiO₂ and CDs-V/TiO₂ composites were dissolved in water at a 5 mg mL^{-1} concentration. Each solution (0.1 mL) was mixed with 0.1 mL of RhB aqueous solution (100 ppm), and 3 mL of deionized water was added. The mixed solutions were then transferred into a quartz cuvette and kept away from any source of light for 1 h with magnetic stirring for the adsorption/desorption equilibrium between catalysts and RhB. Then the solutions were exposed to visible light irradiation with continuous stirring. The decrease in the absorbance

value at the characteristic absorption peak of RhB (554 nm) was measured after irradiation for a constant time interval with visible light. The absorption spectra were measured *in situ* using the absorbance mode of a USB4000-UV-VIS Spectrometer with reference light from an Ocean Optics HL-2000 light source. A 510 nm cut-off filter was placed on the light source to prevent the excitation of CDs-U and CDs-V. The reference light was imported from an Ocean Optics QP8-2-SMA-BX fiber and exported from an Ocean Optics QP1000-2-SR fiber.

Results and discussion

The CDs-V were synthesized according to our previous work with the starting materials of 3 g of citric acid and 6 g of urea.^{12,29} The CDs-V have a specific intrinsic absorption band in the visible region ranging from 400 to 500 nm (Fig. 1a). The mass extinction coefficients of the CDs-V are much higher than those of CdSe/ZnS core/shell quantum dots (QDs) in the entire absorption band, especially in the visible region as shown in Fig. 1a, which indicates that the CDs could be a good photo-sensitive material for PVs. A compact integration of CDs-V with TiO₂ nanoparticles is necessary for efficient electron injection. The CDs-V/TiO₂ composites were prepared by simply mixing them in water under constant stirring for 24 h. The reaction mixtures were diluted with water and centrifuged to remove unadsorbed CDs-V with a speed of 5000 rpm until the supernatant was non-fluorescent. The color of TiO₂ changed from pure white to light brown after the integration of CDs-V with TiO₂ nanoparticles as shown in Fig. S1 (ESI[†]), verifying the success in integrating the CDs-V with TiO₂ nanoparticles. Fig. 1b shows the UV-Vis absorption spectra (converted from diffuse reflection spectra) of TiO₂ and CDs-V/TiO₂ composites. Pure TiO₂ has almost no absorption above 400 nm, while the CDs-V/TiO₂ composites have continuous broad absorption in the visible region ranging from 400 to 600 nm, indicating the adsorption of CDs-V on the surface of TiO₂. To further confirm the integration of CDs-V with TiO₂ nanoparticles, high resolution

transmission electron microscopic (HRTEM) images of the CDs-V/TiO₂ composites were recorded (Fig. 1c and d). As seen from Fig. 1d, the interplanar spacing of 0.35 nm is assigned to the (101) lattice plane of anatase TiO₂, while the 0.21 nm lattice fringes agree well with the (102) plane of graphitic carbon, demonstrating the integration of CDs-V with TiO₂ nanoparticles. It should be mentioned that no long chain molecules were functionalized on the CDs-V. Thus, the cores of the CDs-V could be closely anchored to the surface of TiO₂, resulting in compact integration, as shown in Fig. 1d, which is beneficial for efficient electron injection.

To clearly illustrate the electron injection properties of the CDs-V/TiO₂ composites, the PL properties of the CDs-V/TiO₂ composites in water were studied. The emission of CDs-V could be quenched by TiO₂ after integrating CDs-V with TiO₂. The PL dynamics of CDs-V and CDs-V/TiO₂ composites in water were collected as shown in Fig. 2. After integration with TiO₂ nanoparticles, a shortening in the PL decays of CDs-V was observed. This shortening is ascribed to electron injection from CDs-V to the conduction band of TiO₂.³³ The electron injection rate (k_{EI}) and efficiency (η_{EI}) can be calculated from eqn (1) and (2):

$$k_{\text{EI}} = \frac{1}{\tau_{\text{ave}}(\text{CD} - \text{TiO}_2)} - \frac{1}{\tau_{\text{ave}}(\text{CD})} \quad (1)$$

$$\eta_{\text{EI}} = 1 - \frac{\tau_{\text{ave}}(\text{CD} - \text{TiO}_2)}{\tau_{\text{ave}}(\text{CD})} \quad (2)$$

where $\tau_{\text{ave}}(\text{CD})$ and $\tau_{\text{ave}}(\text{CD}/\text{TiO}_2)$ are the average lifetimes of the CDs-V and CDs-V/TiO₂ composites, respectively.^{33–35} The PL decay curves of the CDs-V and the CDs-V/TiO₂ composites were fitted with bi- or tri-exponential decay kinetics and the calculated k_{EI} and η_{EI} are summarized in Table 1. The k_{EI} and η_{EI} from CDs-V to TiO₂ in water were estimated to be $\sim 0.15 \times 10^8 \text{ s}^{-1}$ and 8.8%, respectively.

To acquire a deep understanding of the electrical interaction between the CDs-V and TiO₂, the PL dynamics of the CDs-V/TiO₂ composites in air were measured, as shown in Fig. 2.

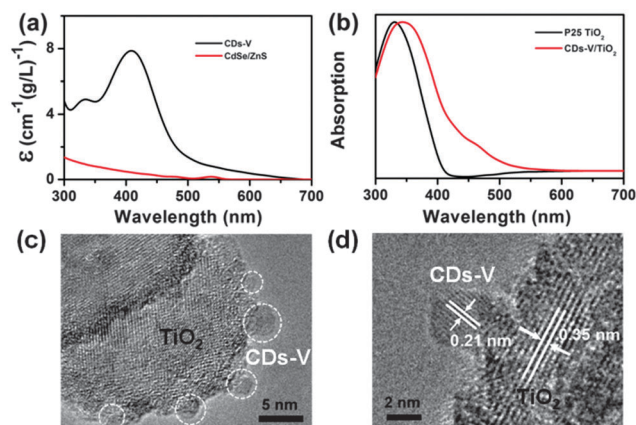


Fig. 1 (a) The mass extinction coefficient spectra of CDs-V in water and CdSe/ZnS core/shell QDs in toluene. (b) Normalized UV-Vis absorption spectra of TiO₂ and CDs-V/TiO₂ composites. HRTEM images of CDs-V/TiO₂ composites (c and d).

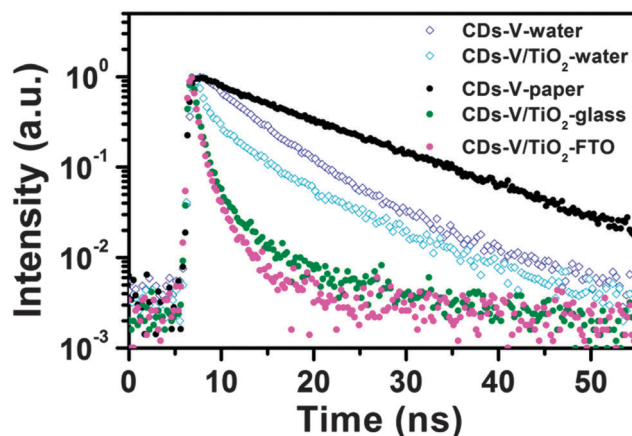


Fig. 2 PL decay curves of the CDs-V and CDs-V/TiO₂ composites in water (empty symbols) and the CDs-V integrated with paper and TiO₂ films on glass and FTO substrates in air (solid symbols), excitation at 405 nm, monitored at 530 nm.

Table 1 Fit parameters of the PL decay curves of the CDs-V and CDs-V/TiO₂ composites in water and CDs-V integrated with paper and TiO₂ films on glass and FTO substrates in air. CDs-V-water and CDs-V-paper are the reference samples in water and air, respectively^a

Samples	τ_1 (ns)	a_1 (%)	τ_2 (ns)	a_2 (%)	τ_3 (ns)	a_3 (%)	χ^2	τ_{ave} (ns)	k_{EI} (10^8 s^{-1})	η_{EI} (%)
CDs-V-water	4.96	74.70	11.02	25.30			1.42	6.49		
CDs-V/TiO ₂ -water	0.60	22.05	4.29	40.14	10.75	37.81	1.25	5.92	0.15	8.8
CDs-V-paper	5.37	11.55	13.10	88.45			1.06	12.20		
CDs-V/TiO ₂ -glass	0.24	50.01	1.51	34.02	9.42	15.97	1.21	2.14	3.9	82
CDs-V/TiO ₂ -FTO	0.15	52.25	1.02	35.40	4.89	12.35	1.12	1.04	8.8	91

^a The average lifetimes were calculated using the equation $\tau_{\text{ave}} = \sum_{i=1}^n a_i \tau_i$.^{36,37}

The CDs-V/TiO₂ composites were prepared by immersing mesoporous TiO₂ films on glass or FTO substrates in aqueous solution of the CDs-V with a concentration of 5 mg mL⁻¹ for 24 h and then rinsing thoroughly with water to avoid the aggregation of CDs-V. The CDs could be separately adsorbed on paper with enhanced fluorescence as shown in our previous report.¹² The reference sample was prepared by dispersing the aqueous solution of the CDs-V with low concentration on commercially available filter paper, which is an insulator and there is no electron transfer process in the CDs-V/paper composites. As seen from Fig. 2, the PL decay of the CDs-V/TiO₂ composites on the glass substrate is significantly shortened, which can be further shortened in the CDs-V/TiO₂ composites on the FTO substrate. The k_{EI} and η_{EI} for the CDs-V/TiO₂ composites on the glass substrate in air were $3.9 \times 10^8 \text{ s}^{-1}$ and 82%, respectively. When the CDs-V were integrated with the TiO₂ film on the conductive FTO substrate, k_{EI} and η_{EI} were further increased to $8.8 \times 10^8 \text{ s}^{-1}$ and 91%. These results demonstrate that efficient electron injection in the CDs-V/TiO₂ composites can be achieved. k_{EI} and η_{EI} from the CDs-V to TiO₂ in water were estimated to be $\sim 0.15 \times 10^8 \text{ s}^{-1}$ and 8.8%, respectively, which were much lower than those for the CDs-V/TiO₂ composites in air. There are three possible dissipative channels for the electrons in the conduction band of TiO₂ in the CDs-V/TiO₂ composites, which are electron extraction by O₂,¹⁶ electron capture by defect states in TiO₂, and electron recombination from TiO₂ to the CDs-V, as shown in Fig. 3. It can be inferred that the content of O₂ in

air is much higher than that in water, which could efficiently extract the photoinduced injected electrons in the conduction band of TiO₂ from the CDs-V. The photoinduced injected electrons in the conduction band of TiO₂ from the CDs-V could not be efficiently extracted by O₂ in water, due to low concentration of O₂ in water ($\sim 8 \text{ mg L}^{-1}$). So the electron injection from the CDs-V to TiO₂ in water was less efficient than that in the composites in air. It can be concluded that the electron capture by defect states in TiO₂ and electron recombination from TiO₂ to the CDs-V are unfavorable compared with electron extraction by O₂. Effective electron capture by defect states in TiO₂ and electron recombination from TiO₂ to the CDs-V would also extract the photoinduced injected electrons in the conduction band of TiO₂ and then promote the electron injection from CDs-V to TiO₂ nanoparticles, which cannot lead to such obvious oxygen-content-dependent electron injection properties. After replacing the glass substrate with the conductive FTO substrate in the CDs-V/TiO₂ composites, k_{EI} and η_{EI} in air were further increased. This is because the FTO substrate enhances the electron extraction from the conduction band of TiO₂ due to the role of the FTO conductive film as another dissipative channel for the electrons. It can be inferred that the visible photoinduced charges in the CDs-V/TiO₂ composites could be efficiently separated and collected through an effective loop in the CD-based PVs.

We further investigated the photoinduced charge separation processes in the CDs-V/TiO₂ composites by photocatalytic experiments on the CDs-V/TiO₂ composites. The decomposition rates of RhB by the CDs-V/TiO₂ composites were measured under visible light irradiation ($\lambda > 400 \text{ nm}$). The absorption spectra of RhB solutions mixed with pure TiO₂ and the CDs-V/TiO₂ composites measured at different visible light irradiation times are shown in Fig. S2a–e (ESI†). The characteristic absorption peak of RhB aqueous solution (554 nm) mixed with CDs-V/TiO₂ composites decreased quickly with peak wavelength exhibiting a blue shift under visible light irradiation (Fig. S2e, ESI†), which might be due to two concomitant photodegradation processes: cleavage of the conjugated chromophore ring structure and de-ethylation of RhB.^{38,39} The intensity ratios of the characteristic absorption peak of RhB (554 nm) after irradiation under visible light for a constant time interval (C) and prior to irradiation (C_0) were calculated as shown in Fig. 4a. Fig. 4b shows the photodegradation kinetics ($\ln(C_0/C)$) of RhB solutions containing different components.¹⁶ As seen from Fig. 4a and b, pure CDs-V have almost no degradation of RhB under visible light. The decomposition rate constant of RhB by the

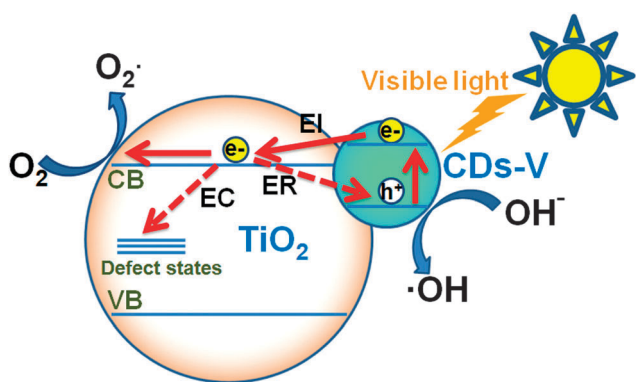


Fig. 3 Schematic illustration for the visible photoinduced electron injection (EI) and possible dissipative channels for the photoinduced electrons in the CDs-V/TiO₂ composites (electron extraction by O₂, electron capture by defect states in TiO₂ (EC) and electron recombination from TiO₂ to the CDs-V (ER)) under visible light irradiation. CB: the conduction band of TiO₂, VB: the valence band of TiO₂.

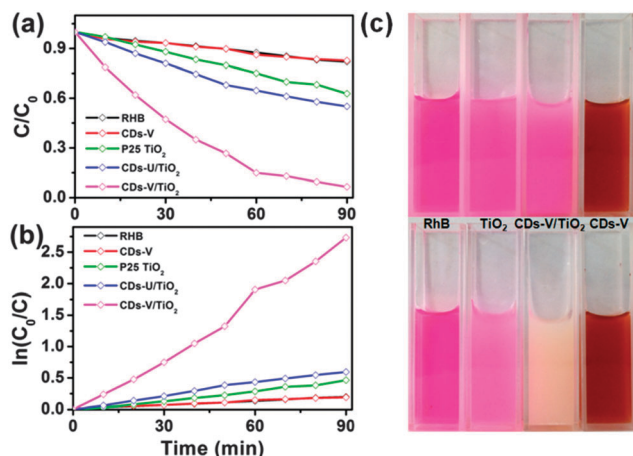


Fig. 4 Photocatalytic performances of the CDs-V, TiO_2 , CDs-U/ TiO_2 and CDs-V/ TiO_2 composites under visible light ($\lambda > 400 \text{ nm}$) (a and b). (c) Optical images of RhB (10 ppm) and mixed solutions of RhB (10 ppm) with pure TiO_2 , the CDs-V/ TiO_2 composites, and CDs-V (TiO_2 , CDs-V/ TiO_2 composites, and CDs-V at the same concentration of 0.5 mg mL^{-1}) without (above) and with (below) daylight irradiation for 2 hours. The pH values of the RhB and mixed solutions of RhB with CDs-V, TiO_2 , CDs-U/ TiO_2 and CDs-V/ TiO_2 composites: 6.51, 6.42, 6.14, 6.32, and 6.47, respectively. Illumination intensity at the solution surface: 72.5 mW cm^{-2} , irradiating area: 1 cm^2 .

CDs-V/ TiO_2 composites was much higher than that of pure TiO_2 , which indicates that the charge separation in the CDs-V/ TiO_2 composites was the major factor for improving the photocatalytic activity of TiO_2 .^{16–19} The photocatalytic activity of the composites based on CDs-U was also investigated (Fig. 4a and b). The CDs-U were synthesized according to recent work.¹⁶ The CDs-U/ TiO_2 composites were prepared using the same method as for CDs-V/ TiO_2 composites. The decomposition rate constant of RhB by the CDs-U/ TiO_2 composites was similar to that of pure TiO_2 and much inferior to that of CDs-V/ TiO_2 composites, due to weak absorption of CDs-U in the visible region (Fig. S2f, ESI†). It can be concluded that the CDs with main absorption in the visible region are important for charge separation in the CDs-V/ TiO_2 composites under visible light to improve the photocatalytic activity of TiO_2 . Fig. 4c shows the optical images of RhB solution and mixed solutions of RhB with pure TiO_2 , the CDs-V/ TiO_2 composites, and the CDs-V without and with sunlight irradiation for 2 hours. It can be seen that most RhB was degraded by the CDs-V/ TiO_2 composites under sunlight for 2 hours, which is much more efficient than pure TiO_2 . The excellent photocatalytic activity of the CDs-V/ TiO_2 composites indicates that the small amount of O_2 and OH^- in water can effectively extract the visible photoinduced electrons and holes in the CDs-V/ TiO_2 composites, respectively, to generate O_2^\bullet and $^\bullet\text{OH}$ to decompose RhB as shown in Fig. 3. It also agrees with the fact that electron recombination from TiO_2 to the CDs-V is unfavorable. It can also be inferred that the visible photoinduced charges in the CDs-V/ TiO_2 composites could be efficiently separated and collected through an effective loop in the CD-based PVs.

Simple CD-sensitized TiO_2 solar cells with a general dye-sensitized solar cell structure with an I^-/I_3^- electrolyte were prepared to further investigate the photoinduced charge separation

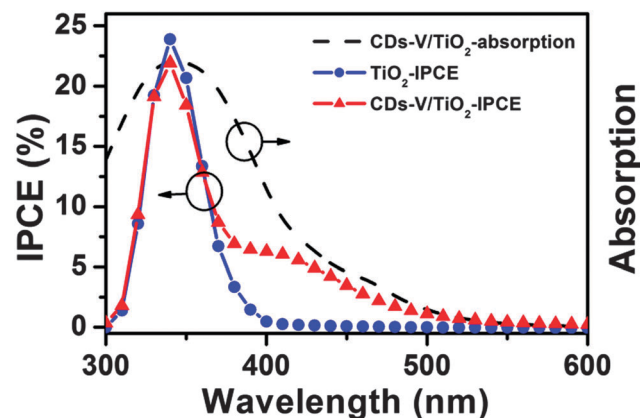


Fig. 5 The IPCE spectra of pure TiO_2 and the CD-sensitized TiO_2 solar cells and UV-Vis absorption spectrum of CDs-V/ TiO_2 composites.

behaviors between CDs-V and TiO_2 . The IPCE spectra of pure TiO_2 and the CD-sensitized TiO_2 solar cells were measured as shown in Fig. 5. The IPCE curve of pure TiO_2 solar cells is almost zero in the visible region ($\lambda > 400 \text{ nm}$) due to the large band gap width of TiO_2 . In comparison, the IPCE curve of the CD-sensitized TiO_2 solar cells is obviously enhanced in the range from 380 to 500 nm, indicating that the visible absorption of CDs-V contributes to the photogenerated current. At this stage, the performance of the CD-sensitized TiO_2 solar cells is unsatisfactory, which might be due to the low adsorption degree of the CDs-V on the TiO_2 electrode causing low absorption of visible light as evaluated from the UV-Vis absorption spectrum of the CDs-V/ TiO_2 composites, in which the relative intensity of CDs-V and TiO_2 is low (Fig. 5). Considering the relatively low adsorption degree of CDs-V on the TiO_2 electrode and the similar shapes of the IPCE spectrum of the CD-sensitized TiO_2 solar cell and the absorption spectrum of CDs-V/ TiO_2 composites, the photoinduced charge separation between CDs-V and the TiO_2 electrode should be efficient. We propose that the performance of the CD-sensitized TiO_2 solar cells can be further improved by increasing the adsorption degree of the CDs-V on the TiO_2 electrode, and this work is in process.

Conclusions

In summary, non-long-chain-molecule-functionlized CDs with visible intrinsic absorption (CDs-V) were compactly integrated with TiO_2 . The PL dynamics study demonstrated that photo-generated electrons from the CDs-V could quickly and efficiently inject into TiO_2 with $k_{\text{EI}} = 8.8 \times 10^8 \text{ s}^{-1}$ and $\eta_{\text{EI}} = 91\%$, respectively, in the CDs-V/ TiO_2 composites. The CDs-V/ TiO_2 composites exhibited excellent photocatalytic activity under visible light, which was much better than pure TiO_2 and CDs-U/ TiO_2 composites, indicating that visible photoinduced electrons and holes in CDs-V/ TiO_2 composites could be effectively separated and electron recombination from TiO_2 to the CDs-V was unfavorable. The IPCE results for the CD-sensitized TiO_2 solar cells also agreed with efficient photoinduced charge separation between CDs-V and the TiO_2 electrode in the visible range. These results demonstrate that the non-long-chain-molecule-functionlized

CDs with a visible intrinsic absorption band are appropriate candidates as photosensitizers and indicate that the visible photoinduced charges in the CDs-V/TiO₂ composites could be efficiently separated and collected through an effective loop in the CD-based PV system.

Acknowledgements

We thank Prof. Xinhua Zhong of East China University of Science and Technology for preparing the CD-sensitized TiO₂ solar cells and measuring the IPCE results. This work was supported by the National Science Foundation of China No. 11204298, 61205025, 61274126, the Jilin Province Science and Technology Research Project No. 20140101060JC, 20150519003JH, the Outstanding Young Scientist Program of CAS, and a project supported by the State Key Laboratory of Luminescence and Applications.

Notes and references

- 1 L. Cao, M. J. Meziani, S. Sahu and Y. Sun, *Acc. Chem. Res.*, 2013, **46**, 171.
- 2 S. Zhu, Q. Meng, L. Wang, J. Zhang, Y. Song, H. Jin, K. Zhang, H. Sun, H. Wang and B. Yang, *Angew. Chem., Int. Ed.*, 2013, **125**, 1.
- 3 T. Yeh, C. Teng, S. Chen and H. Teng, *Adv. Mater.*, 2014, **26**, 3297.
- 4 K. Kalyanasundaram and M. Grätzel, *J. Mater. Chem.*, 2012, **22**, 24190.
- 5 W. Wei, C. Xu, L. Wu, J. Wang, J. Ren and X. Qu, *Sci. Rep.*, 2014, **4**, 3564.
- 6 C. Ding, A. Zhu and Y. Tian, *Acc. Chem. Res.*, 2014, **47**, 20.
- 7 S. Zhuo, M. Shao and S. Lee, *ACS Nano*, 2012, **6**, 1059.
- 8 K. J. Williams, C. A. Nelson, X. Yan, L. Li and X. Zhu, *ACS Nano*, 2013, **7**, 1388.
- 9 H. Choi, S. Ko, Y. Choi, P. Joo, T. Kim, B. R. Lee, J. Jung, H. J. Choi, M. Cha, J. Jeong, I. Hwang, M. H. Song, B. Kim and J. Y. Kim, *Nat. Photonics*, 2013, **7**, 732.
- 10 H. Li, Z. Kang, Y. Liu and S. Lee, *J. Mater. Chem.*, 2012, **22**, 24230.
- 11 Y. Sun, B. Zhou, Y. Lin, W. Wang, K. A. S. Fernando, P. Pathak, M. J. Meziani, B. A. Harruff, X. Wang, H. Wang, P. G. Luo, H. Yang, M. E. Kose, B. Chen, L. M. Veca and S. Xie, *J. Am. Chem. Soc.*, 2006, **128**, 7756.
- 12 S. Qu, X. Wang, Q. Lu, X. Liu and L. Wang, *Angew. Chem., Int. Ed.*, 2012, **51**, 12215.
- 13 S. Qu, D. Shen, X. Liu, P. Jing, L. Zhang, W. Ji, H. Zhao, X. Fan and H. Zhang, *Part. Part. Syst. Charact.*, 2014, **31**, 1175.
- 14 X. Li, Y. Liu, X. Song, H. Wang, H. Gu and H. Zeng, *Angew. Chem., Int. Ed.*, 2015, **54**, 1759.
- 15 X. Li, S. Zhang, S. A. Kulinich, Y. Liu and H. Zeng, *Sci. Rep.*, 2014, **4**, 4976.
- 16 D. Qu, M. Zheng, P. Du, Y. Zhou, L. Zhang, D. Li, H. Tan, Z. Zhao, Z. Xie and Z. Sun, *Nanoscale*, 2013, **5**, 12272.
- 17 H. Yu, Y. Zhao, C. Zhou, L. Shang, Y. Peng, Y. Cao, L. Wu, C. Tung and T. Zhang, *J. Mater. Chem. A*, 2014, **2**, 3344.
- 18 S. T. Kochuveedu, Y. J. Jang, Y. H. Jang, W. J. Lee, M. Cha, H. Shin, S. Yoon, S. Lee, S. O. Kim, K. Shin, M. Steinhart and D. H. Kim, *Green Chem.*, 2011, **13**, 3397.
- 19 G. Cui, W. Wang, M. Ma, M. Zhang, X. Xia, F. Han, X. Shi, Y. Zhao, Y. Dong and B. Tang, *Chem. Commun.*, 2013, **49**, 6415.
- 20 J. Bian, C. Huang, L. Wang, T. Hung, W. A. Daoud and R. Zhang, *ACS Appl. Mater. Interfaces*, 2014, **6**, 4883.
- 21 P. Mirtchev, E. J. Henderson, N. Soheilnia, C. M. Yip and G. A. Ozin, *J. Mater. Chem.*, 2012, **22**, 1265.
- 22 P. V. Kamat, *Acc. Chem. Res.*, 2012, **45**, 1906.
- 23 P. V. Kamat, K. Tvrđy, D. R. Baker and J. G. Radich, *Chem. Rev.*, 2010, **110**, 6664.
- 24 F. Liu, M. Jang, H. D. Ha, J. Kim, Y. Cho and T. S. Seo, *Adv. Mater.*, 2013, **25**, 3657.
- 25 S. Zhu, J. Zhang, S. Tang, C. Qiao, L. Wang, H. Wang, X. Liu, B. Li, Y. Li, W. Yu, X. Wang, H. Sun and B. Yang, *Adv. Funct. Mater.*, 2012, **22**, 4732.
- 26 Z. Yang, C. Chen, P. Roy and H. Chang, *Chem. Commun.*, 2011, **47**, 9561.
- 27 M. Graetzel, R. A. J. Janssen, D. B. Mitzi and E. H. Sargent, *Nature*, 2012, **488**, 304.
- 28 F. Hetsch, X. Xu, H. Wang, S. V. Kershaw and A. L. Rogach, *J. Phys. Chem. Lett.*, 2011, **2**, 1879.
- 29 S. Qu, X. Liu, X. Guo, M. Chu, L. Zhang and D. Shen, *Adv. Funct. Mater.*, 2014, **24**, 2689.
- 30 F. Wang, Y. Chen, C. Liu and D. Ma, *Chem. Commun.*, 2011, **47**, 3502.
- 31 S. Qu, H. Chen, X. Zheng, J. Cao and X. Liu, *Nanoscale*, 2013, **5**, 5514.
- 32 Q. Lou, S. Qu, P. Jing, W. Ji, D. Li, J. Cao, H. Zhang, L. Liu, J. Zhao and D. Shen, *Adv. Mater.*, 2015, **27**, 1315.
- 33 A. Kongkanand, K. Tvrđy, K. Takechi, M. Kuno and P. V. Kamat, *J. Am. Chem. Soc.*, 2008, **130**, 4007.
- 34 M. Abdellah, K. Židek, K. Zheng, P. Chábera, M. E. Messing and T. Pullerits, *J. Phys. Chem. Lett.*, 2013, **4**, 1760.
- 35 J. Sun, J. Zhao and Y. Masumoto, *Appl. Phys. Lett.*, 2013, **102**, 053119.
- 36 S. Jin and T. Lian, *Nano Lett.*, 2009, **9**, 2448.
- 37 M. Y. Berezin and S. Achilefu, *Chem. Rev.*, 2010, **110**, 2641.
- 38 T. Wu, G. Liu, J. Zhao, H. Hidaka and N. Serpone, *J. Phys. Chem. B*, 1998, **102**, 5845.
- 39 H. Fu, S. Zhang, T. Xu, Y. Zhu and J. Chen, *Environ. Sci. Technol.*, 2008, **42**, 2085.